

1 **Effects of Urbanization on the water cycle in the Shiyang River**  
2 **Basin: Based on stable isotope method**

3 Rui Li<sup>a,b</sup>, Guofeng Zhu<sup>a,b,\*</sup>, Siyu Lu<sup>a,b</sup>, Liyuan Sang<sup>a,b</sup>, Gaojia Meng<sup>a,b</sup>, Longhu Chen<sup>a,b</sup>,  
4 Yinying Jiao<sup>a,b</sup>, Qinqin Wang<sup>a,b</sup>

5 **Affiliations:**

6 <sup>a</sup> *College of Geography and Environmental Science, Northwest Normal University, Lanzhou*  
7 *730070, Gansu, China*

8 <sup>b</sup> *Shiyang River Ecological Environment Observation Station, Northwest Normal University,*  
9 *Lanzhou 730070, Gansu, China*

10 *\*Corresponding author. Email: zhugf@nwnu.edu.cn.*

11 **Abstract:** In water-scarce arid areas, the water cycle is affected by urban  
12 development and natural surface changes, and urbanization has a profound impact on  
13 the hydrological system of the basin. Through an ecohydrological observation system  
14 established in the Shiyang River basin in the inland arid zone, we studied the impact of  
15 urbanization on the water cycle of the basin using isotope methods. The results  
16 showed that urbanization significantly changed the water cycle process in the basin,  
17 and accelerated the rainfall-runoff process due to the increase of urban land area, and  
18 the mean residence time (MRT) of river water showed a fluctuating downward trend  
19 from upstream to downstream, and was shortest in the urban area in the middle  
20 reaches, and the MRT was mainly controlled by the landscape characteristics of the  
21 basin. In addition, our study showed that river water and groundwater isotope data  
22 were progressively enriched from upstream to downstream due to the construction of  
23 metropolitan landscape dams, which exacerbated evaporative losses of river water, and

24 also strengthened the hydraulic connection between groundwater and river water  
25 around the city. Our findings have important implications for local water resource  
26 management and urban planning and provide important insights into the hydrologic  
27 dynamics of urban areas.

28 **Keywords:** Urbanization; Water cycle; Stable isotopes; River Connectivity

## 29 **1 Introduction**

30 According to the "2020 Global Cities Report," urban areas are currently home to  
31 more than half of the worldwide people, which amounts to 56.2%. This pattern is  
32 expected to continue over the course of the next decade, culminating in an  
33 urbanization rate of 60.4% by the year 2030. In addition, the study forecasts that by  
34 the year 2050, approximately seventy percent of the world's population would reside  
35 in urban areas (Chen et al., 2020; UN, 2019; UN-Habitat, 2020). Unlike other regions,  
36 urban regions have a substantial influence on the hydrological system, resulting in  
37 significant consequences on water balance and the water cycle (Gillefalk et al., 2021).  
38 To meet the diverse household and industrial requirements in metropolitan areas,  
39 where the population is concentrated and water demands are high, a complex  
40 interplay between natural and manmade components of the water cycle is required.  
41 These components include both natural features such as streams and groundwater, as  
42 well as human-made systems like drinking water and drainage networks (Gessner et  
43 al., 2014). Urbanization exacerbates water depletion and has far-reaching impacts on  
44 groundwater (Flörke et al., 2018; McDonough et al., 2020), affecting the environment  
45 and water availability (Bhaskar and Welty, 2015). Rapid urbanization will seriously

46 pressure the structure, function and water quality degradation of basin ecosystems  
47 (Grimm et al., 2008; Sun and Lockaby, 2012; Sun et al., 2015).

48 Urbanization's effects on basin hydrology and the related processes have  
49 complex and varying consequences (Caldwell et al., 2012; Martin et al., 2017). In the  
50 past few decades, with the continuous acceleration of urbanization, human activities  
51 in urban areas have become more frequent, and the hydrological effects of  
52 urbanization have become more intense, attracting widespread attention worldwide  
53 (Salvadore et al., 2015). The rise of impervious surfaces in urbanized regions  
54 increases the rate of urban water runoff, which raises the danger of urban floods  
55 (Wing et al., 2018). In addition, high-intensity human activities have led to increased  
56 discharge of domestic sewage and industrial wastewater, deteriorating water quality  
57 and ecological environment (Pickett et al., 2011). Meanwhile, basin water cycle  
58 processes are influenced by a combination of meteorological and subsurface factors. It  
59 has been found that urbanization has led to significant increases in runoff and peak  
60 flows in rivers (Liu et al., 2018; Han et al., 2022) and has resulted in shorter runoff  
61 response times (Anderson et al., 2022), which also exacerbates the intensity and  
62 frequency of flooding in basins (De Niel and Willems, 2019; Blum et al., 2020). On  
63 the other hand, the urbanization process leads to an increase in the amount of rainfall  
64 in the basin as well as an increase in the frequency of extreme rainfall events (Shastri  
65 et al., 2015; Fu et al., 2019; Yang et al., 2021), whereas in dryland inland river basins  
66 in arid zones that are dependent on water resources for development, the impacts of  
67 urbanization on the water cycle processes of the basins are still not clear, and they

68 need to be explored in depth the effects of urbanization on basin water cycle processes.  
69 Hence, study into how human activities alter the features of river runoff and the water  
70 cycle within a basin is essential for the prudent use and sustainable development of  
71 water resources.

72 Isotopes that are stable of hydrogen and oxygen are very useful tools for  
73 investigating hydrological issues that are connected to surface water and groundwater  
74 sources (Fekete et al., 2006; Förstel and Hützen, 1983; Vystavna et al., 2021).  
75 Researchers have been conducting studies using stable isotopes as tracers over the  
76 course of the past few years in order to explore the impact that urbanization has had  
77 on the water cycle. Urbanization has the potential to trigger and intensify convective  
78 activity and warm-season rainfall in both urban areas and their surrounding regions  
79 (Burian and Shepherd, 2005). Researchers generally agree that urbanization reduces  
80 depressions on the underlying surface, weakens water permeability and increases  
81 runoff. At the same time, the lower roughness of the underlying surface shortens the  
82 confluence time (Guan et al., 2015; Oudin et al., 2018). Moreover, against the  
83 backdrop of swift urbanization, the swift proliferation of urban regions has resulted in  
84 a sharp surge in impermeable areas, alterations to regional microclimates, and the  
85 erection of a vast number of infrastructures (including overpasses, subways, and so  
86 on), all of which have significantly impacted the water cycle process in urban areas  
87 (Jacobson, 2011; Westra et al., 2014). The complex connection between the permeable  
88 and impermeable zones influences the surface confluence processes (Bruwier et al.,  
89 2020). The construction of urban water conservation projects, such as rubber dams

90 and pumping stations, also affects the confluence process of urban areas to a certain  
91 extent (Zhu et al., 2021). Limited long-term and continuous monitoring has hampered  
92 accurate depiction of urbanization's spatiotemporal effects on basin hydrology.  
93 Furthermore, the scientific research till lacks sufficient research on arid regions that  
94 heavily depend on mountain river runoff for sustenance and development.

95       Against the background of increasing urbanization, it is particularly important to  
96 study the hydrological impacts of urbanization on basins and their corresponding  
97 countermeasures, especially in arid inland river basins, where the impacts of human  
98 activities in urban areas on rivers may be more prominent. Therefore, the Shiyang  
99 River Basin (SYR), located in the inland arid zone of Northwest China, was used as  
100 an example to study the impact of urbanization on the hydrology of the basin using  
101 the stable isotope method. The following problems are proposed to be solved: (1) An  
102 examination of the mechanisms underlying evaporation and infiltration of surface  
103 water within urban aquatic ecosystems; (2) Assessing the effects of urbanization on  
104 water body connectivity through a comprehensive analysis; (3) The influence of  
105 urbanization on the precipitation-runoff process is analyzed. This provides us with  
106 essential information on how to maintain and manage the water resources found in  
107 inland river basins, which is especially useful in light of the fact that the rate of  
108 urbanization is growing.

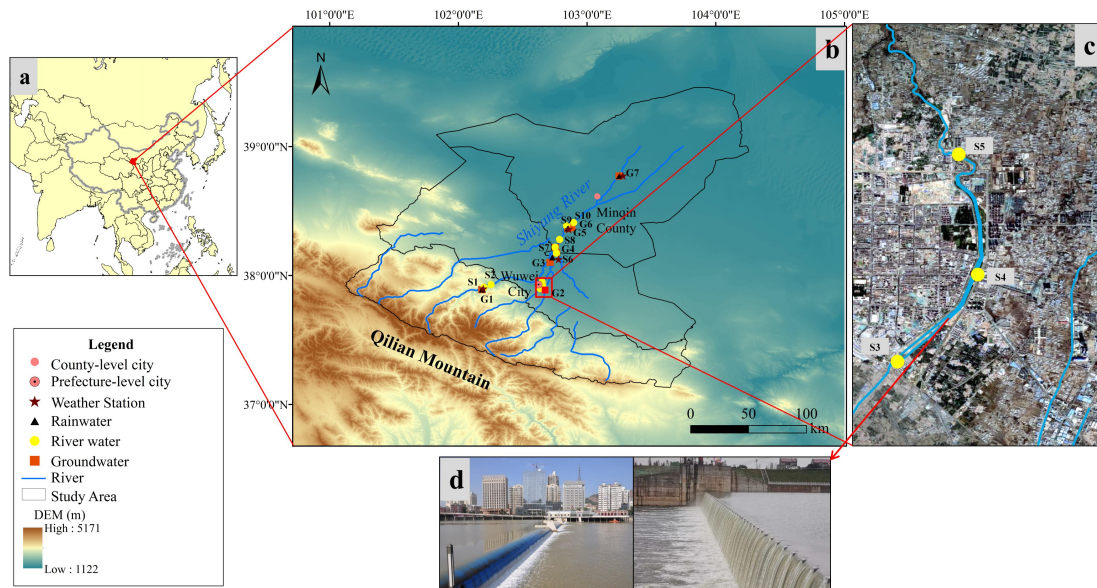
## 109 **2 Systems, Data, and Methods of Observation**

110       The SYR Basin is located in Gansu Province, China, to the east of the He-xi  
111 Corridor. Its coordinates are 101°22' ~ 104°16' E and 36°29' ~ 39°27' N. The SYR

112 Basin is bounded to the west by the Wushaoling Mountain and to the north by the  
113 foothills of the Qilian Mountain (Zhu et al., 2019). The basin in question is situated  
114 within the continental temperate belt, characterized by a parched climate and diverse  
115 topography. Annual precipitation hovers within the range of 100 to 600 mm, while  
116 pan evaporation levels exhibit greater variability, ranging from 700 to 2600 mm  
117 annually. The majesty of the Qilian Mountains is where the SYR begins its journey,  
118 and the Qilian Mountains are the source of its eight main tributaries. The SYR is  
119 principally supported by the convergence of precipitation, snowmelt, and glacier  
120 runoff (Wei et al., 2013).

121 The Wuwei City is crossed by four important rivers, namely the Xiying, Zamu,  
122 Huangyang and Jinta, which cover a catchment area of 3986 km<sup>2</sup>. As the principal  
123 water source for the entire region, the SYR Basin is one of the most highly utilized  
124 inland river basins in terms of water resource development and consumption  
125 worldwide. The dams in the SYR basin are predominantly situated in close proximity  
126 to the urbanized regions of Liangzhou District, located within Wuwei City. Liangzhou  
127 District, situated in the middle of the basin, boasts of a relatively high population  
128 density and a notable commercial concentration. At the turn of the millennium,  
129 Wuwei City only boasted a paltry five landscape dams positioned on its rivers. As of  
130 2019, this figure has surged dramatically, with a staggering total of 51 urban  
131 landscape dams now gracing both urban and peri-urban areas of the city. These dams  
132 are primarily composed of man-made landscape waterfalls and rubber dams, fulfilling  
133 their core function of creating public landscape water bodies within the urban expanse.

134 (Zhu et al ., 2021).



135

136 Figure 1 (a) The location of the study area, (b) Comprehensive observation system for the study

137 area, (c) Urban surface water sampling points (from Google Maps), (d) Common urban landscape

138 dams in SYR Basin.

### 139 3 Sampling and data analysis

140 Since 2017, a comprehensive observation system has been established in the

141 SYR Basin, and stable isotope observations and hydrometeorological observations

142 have been carried out on surface water, shallow groundwater and rainfall. Continuous

143 sampling in the SYR Basin was carried out from April 2017 to March 2021, different

144 water bodies were sampled, and we collected a total of 943 samples from 24 sampling

145 points (Table 1). The river sampling location ought to be selected such that it is

146 physically possible to go as close to the middle of the river as possible, with the goal

147 of minimizing the impact of areas with standing water and sewage. Artesian well

148 water was collected as groundwater samples at 7 sampling locations around the basin.

149 The automated weather station was used to measure meteorological factors such as

150 temperature and relative humidity while collecting precipitation samples. Water  
 151 samples were sealed in high-density polyethylene bottles to avoid evaporation and  
 152 leakage during transit and storage, precipitation samples were collected using weather  
 153 station standard rain gauges. These samples were then frozen and wrapped with  
 154 plastic tape.

155 Table 1 Basic information on precipitation, surface water and groundwater sampling sites

Parameter	Sampling Point	Number	Sampling period	Collection Channels
Precipitation	P1, P2, P3, P4, P5,P6, P7,	387	Precipitation events	Rain tube collection
Surface Water	S1,S2,S3,S4,S5,S6, S7, S8, S9, S10	270	Monthly	Sampling in river water
Groundwater	G1, G2, G3, G4, G5, G6, G7	189	Monthly	Sampling from wells

156 Analysis of the water samples is conducted through liquid water isotope  
 157 analysis utilizing the DLT-100 (Los Gatos Research) in the Stable Isotope Laboratory  
 158 at Northwest Normal University. Each water sample and isotope standard are injected  
 159 six times in succession to assure reliable findings, with the first two injection values  
 160 eliminated and the average of the last four injections used for final analysis, thereby  
 161 avoiding any potential isotope analysis memory effect. The isotope measurements  
 162 were denoted by the symbol " $\delta$ ," which indicates the deviation in thousandths from  
 163 the Vienna Standard Mean Ocean Water:

$$164 \quad \delta_{\text{sample}}(\text{‰}) = \left[ \left( \frac{R_s}{R_{v-smow}} \right) - 1 \right] \times 1000 \quad (1)$$

165 where  $R_s$  is the ratio of  $^{18}\text{O}/^{16}\text{O}$  or  $^2\text{H}/^1\text{H}$  in the collected sample,  $R_{v-smow}$  is the



166 ratio of  $^{18}\text{O}/^{16}\text{O}$  or  $^2\text{H}/^1\text{H}$  of the Vienna standard sample, and the analytical accuracy  
167 of  $\delta\text{D}$  and  $\delta^{18}\text{O}$  is  $\pm 0.6\text{‰}$  and  $\pm 0.2\text{‰}$ , respectively.

### 168 **3 Analysis methods**

#### 169 **3.1 Calculation and indication of *d-excess***

170 Dansgaard (1964) introduced the concept of deuterium excess (*d-excess*) as the  
171 difference in isotopic composition between global precipitation and the Vienna  
172 Standard Mean Ocean Water ( $V_{SMOW}$ ) reference water, which corresponds to a value of  
173 10‰. This parameter reflects the average isotopic composition of air masses  
174 associated with precipitation and is widely used to identify atmospheric source  
175 regions (Deng et al., 2016). *d-excess* was proposed by Dansgaard (Dansgaard, 1964)  
176 and is defined as:

$$177 \quad d\text{-excess} = \delta\text{D} - 8\delta^{18}\text{O} \quad (2)$$

#### 178 **3.2 Calculation of evaporation losses of surface water**

179 The losses of surface water through evaporation and the resulting fluctuations in  
180 water levels of rivers, lakes, and wetlands are key aspects of the terrestrial water cycle  
181 that merit significant attention (Gammons et al., 2006; Hamilton et al., 2005).  
182 Evaporation is the primary mechanism of water losses in the water cycle. For river  
183 water in dry regions and urban river water that flows slowly due to manmade  
184 constraints, evaporation cannot be ignored. Thus, it is vital to address the alteration of  
185 urban landscape dam water caused by non-equilibrium isotope fractionation during  
186 evaporation. The provided formula (3) can be used to estimate the rate of evaporative  
187 water losses from the body of water in question (Skrzypek et al., 2015):

$$f = 1 - \left[ \frac{(\delta - \delta^*)}{(\delta_0 - \delta^*)} \right]^{\frac{1}{m}} \quad (3)$$

188

189 The variables in the equation are as follows:  $f$  represents the ratio of water lost to  
 190 evaporation,  $\delta$  denotes the measured values of the water body located in the urban  
 191 dam area of Wuwei City, situated in the middle reaches of the SYR and  $\delta_0$  represents  
 192 the initial value of the hydrogen and oxygen stable isotope of the water body. It is  
 193 widely assumed that the point of intersection between the local meteoric water line  
 194 (LMWL) and the local evaporation line (LEL) represents the average isotopic  
 195 composition of the input water body within the basin (Gibson et al., 2005). In the  
 196 current investigation, the intersection point marked by  $\delta^{18}\text{O} = -7.24\text{‰}$  and  $\delta\text{D} =$   
 197  $-46.9\text{‰}$  has been designated as the  $\delta_0$  value, while  $\delta^*$  denotes the maximum isotope  
 198 enrichment factor and  $m$  corresponds to the enrichment slope. The calculation of the  
 199 above parameters in this paper is realized in Hydrocalculator software (Skrzypek et al.,  
 200 2015) (<http://hydrocalculator.gskrzypek.com>). According to studies (Qian et al., 2007),  
 201 it is more accurate to use  $\delta^{18}\text{O}$  when calculating the evaporation losses ratio, so this  
 202 study calculates the  $f$  value of SYR water using  $\delta^{18}\text{O}$  value.

### 203 3.3 Periodic regression analysis and the mean residence time (MRT)

204 Seasonal fluctuations in  $\delta^{18}\text{O}$  values were analyzed using periodic regression  
 205 analysis to determine how these values changed over time. This method entailed  
 206 fitting seasonal sine wave curves to annual  $\delta^{18}\text{O}$  variations using least squares  
 207 optimization (Rodgers et al., 2005):

$$\delta^{18}\text{O} = \delta^{18}\text{O}_{ave} + A \cdot [\cos(c \cdot t - \theta)] \quad (4)$$

208

209 The modelled  $\delta^{18}O$  values and the mean weighted annual measured  $\delta^{18}O_{ave}$   
210 values were both utilized in the analysis of seasonal fluctuations in  $\delta^{18}O$  levels.  
211 Additionally, the measured  $\delta^{18}O$  annual amplitude ( $A$ ), the radial frequency of annual  
212 fluctuations ( $c$ ), and the time in days after the start of the sampling period ( $t$ ) were  
213 also considered in this analysis. Furthermore, the phase lag or time of the annual peak  
214  $\delta^{18}O$  in radians ( $\theta$ ) was determined through this approach.

215 An exponential model was used for the purpose of estimating the mean residence  
216 time (MRT). This model operates on the presumption that precipitation inputs quickly  
217 mix with resident water. In order to do this, the following equation was used  
218 (Maloszewski et al., 1983; Rodgers et al., 2005):

$$219 \quad MRT = c^{-1} \cdot \left[ (A_{Z2} / A_{Z1})^{-2} - 1 \right]^{0.5} \quad (5)$$

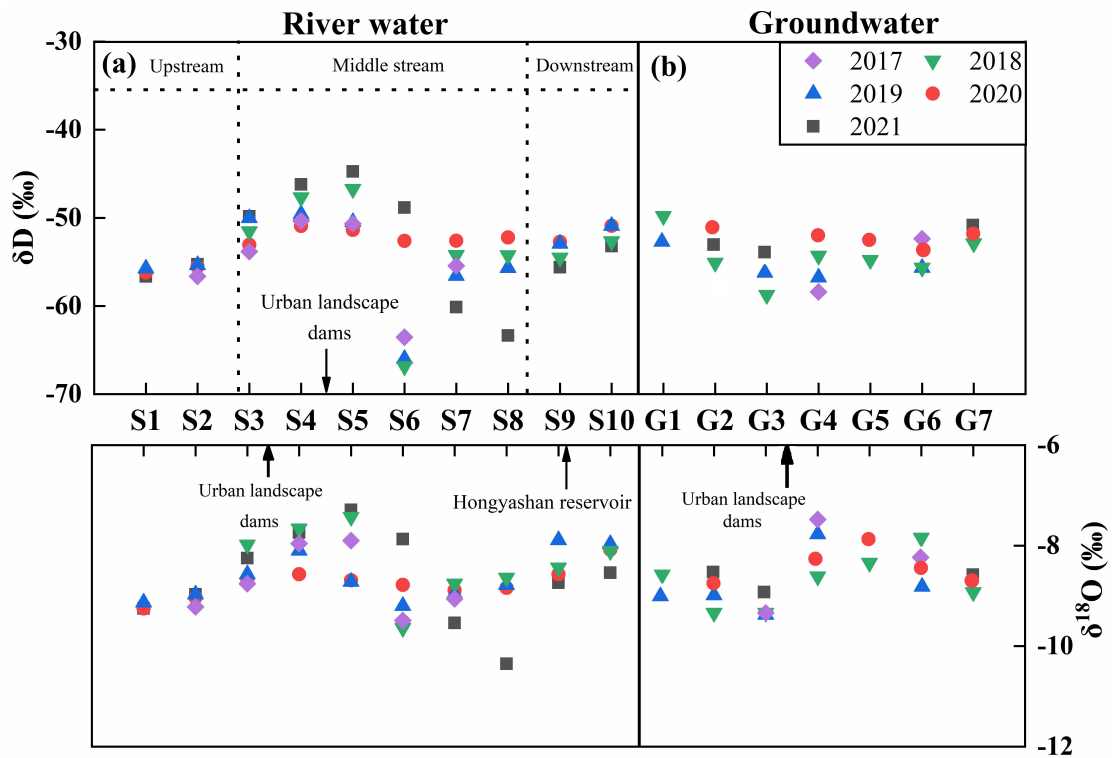
220 The amplitude of precipitation ( $A_{Z1}$ ), the amplitude of the surface water outputs  
221 ( $A_{Z2}$ ), and the radial frequency of the annual fluctuation ( $c$ ) as defined in Eq. (4) were  
222 taken into consideration to estimate the mean residence time (MRT).

## 223 **4 Results**

### 224 **4.1 Spatiotemporal distribution of isotopes in different water bodies**

225 The isotopes values of the surface water in the SYR Basin show a clear  
226 enrichment from upstream to downstream when viewed from space. It is worth noting  
227 that landscape dams and reservoirs in urban areas alter this pattern significantly,  
228 producing markedly higher isotopic compositions of surface water around such  
229 structures (Fig. 2). To be more specific, the surface water throughout the entire basin  
230 had average isotope values that were lower than those of the sampling points in the  
231 dams region, which had values that were greater (Table 2). In addition, the dams

232 slowed the flow of the river, this resulted in isotope enrichment of the river water.  
 233 Notably, these values exhibit spatial and temporal variability, with the largest  $\delta D$  and  
 234  $\delta^{18}O$  values observed in river water, and the lowest in groundwater.



235  
 236 Figure 2 Longitudinal variation of  $\delta D$  and  $\delta^{18}O$  in river water and groundwater in the SYR Basin.

237 To be more specific, over the course of time, these values shift seasonally from  
 238 spring to autumn (Table 2, Fig. 3). There was a range of values from -75.43‰ to  
 239 -40.62‰ for the  $\delta D$  values of surface water, with an average of -53.53‰. The  $\delta^{18}O$   
 240 values display a varied range, from -10.43‰ to -5.53‰, with an average of -8.54‰,  
 241 whereas the *d-excess* values demonstrate variability ranging from 10.26‰ to 29.72‰,  
 242 with 15.28‰ as the average value. A broad spectrum of  $\delta D$  values are observed  
 243 during the summer season, ranging from -61.27‰ to -31.16‰, with an average  
 244 -48.90‰. Meanwhile,  $\delta^{18}O$  values fluctuate between -9.52‰ and -3.41‰, with an  
 245 average -8.12‰. The phenomenon that was observed can be traced back primarily to

246 the aftereffects of the Hongyashan Reservoir built downstream. Because the reservoir  
 247 has such a large capacity for water retention, it causes significant amounts of river  
 248 water to evaporate in summer, which ultimately results in a discernible enrichment of  
 249 the isotopic composition. In both surface water and groundwater,  $\delta D$  and  $\delta^{18}O$  showed  
 250 significant seasonal variations (Fig. 3). Seasonal variations were more pronounced in  
 251 surface water than in groundwater, with surface water showing the largest amplitude  
 252 in spring and the smallest amplitude in fall, while groundwater showed closer  
 253 amplitudes in all seasons, which also indicates that groundwater is less disturbed.

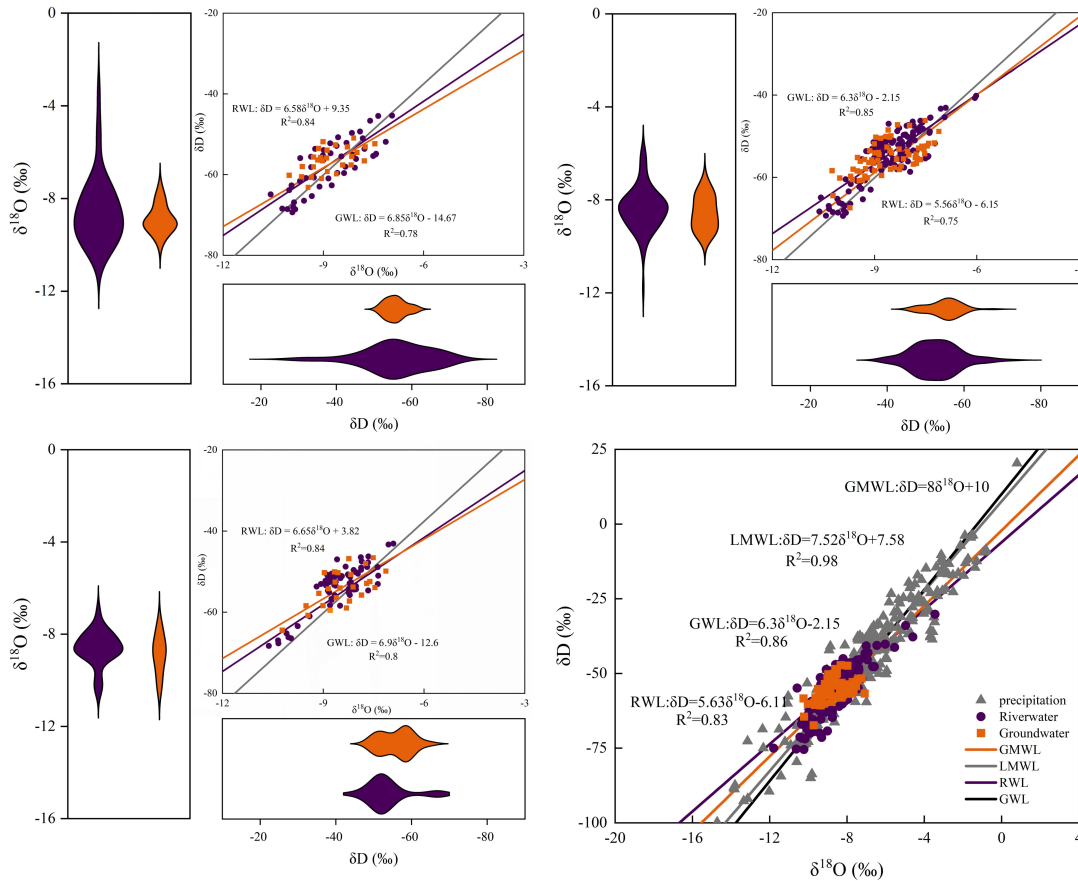
254 Table 2 Isotopic composition statistics of surface water in SYR Basin

Sampling Point	$\delta^{18}O$			$\delta D$			<i>d-excess</i>		
	Mean	Min.	Max.	Mean	Min.	Max.	Mean	Min.	Max.
S1	-9.35	-9.86	-9.06	-57.16	-59.46	-52.47	17.2	12.33	23.91
S2	-9.22	-10.02	-8.78	-56.62	-63.85	-10.02	16.46	15.53	19.28
S3	-7.74	-9.03	-7.75	-49.84	-50.76	-46.66	15.42	13.59	19.48
S4	-7.29	-8.79	-7.65	-46.22	-53.29	-46.26	14.9	11.01	18.03
S5	-7.43	-9.11	-5.53	-48.84	-56.66	-40.62	14.29	14.21	29.72
S6	-9.54	-10.43	-8.29	-60.14	-75.43	-54.40	14.31	10.26	17.62
S7	-9.04	-9.54	-8.21	-54.23	-70.04	-48.03	16.54	12.81	21.16
S8	-9.15	-10.35	-8.64	-56.37	-63.35	-52.22	16.84	14.56	19.54
S9	-8.41	-9.70	-6.02	-53.95	-65.33	-45.54	13.33	12.31	19.50
S10	-8.18	-8.84	-6.58	-51.92	-58.05	-45.39	13.48	12.21	21.72

#### 256 4.2 The Relationship between $\delta D$ and $\delta^{18}O$ values

257 As shown by the linear fitting equation  $\delta D = 7.52\delta^{18}O + 7.58$ , there is a significant  
 258 linear positive correlation ( $R^2 = 0.96$ ) between  $\delta D$  and  $\delta^{18}O$  in atmospheric  
 259 precipitation in the SYR Basin (Fig. 3). It is clear that the slope (7.52) and intercept  
 260 (7.58) of the local meteoric water line (LMWL) are smaller than the global meteoric  
 261 water line (GMWL), which can be attributed to the basin's location in an inland arid  
 262 region, where precipitation disturbances are less frequent and evaporative

263 fractionation of precipitation is stronger. On the other hand, compared with the slopes  
264 of the LMWL, the slopes of the surface water line (SWL) and the groundwater line  
265 (GWL) are relatively close (Fig. 3), indicating that there is a strong hydraulic  
266 connection between groundwater and river water in the SYR basin, and the slopes of  
267 GWL and RWL show  $GWL > RWL$  in all seasons, suggesting that the river water is  
268 most affected by evaporation and groundwater is less affected by evaporation. In  
269 addition, both surface water and groundwater sampling points were distributed near  
270 the LMWL, indicating that both river water and groundwater receive recharge from  
271 precipitation. Overall, the H-O isotopic composition of surface water samples from  
272 the SYR showed a linear regression of  $\delta D = 5.63\delta^{18}O - 6.11$ , and the slope of RWL  
273 was the largest in the autumn (slope = 6.65) and the smallest in the summer (slope =  
274 5.56), which indicated that the river water evaporated the weakest in the autumn and  
275 the strongest in the summer.



276

277 Figure 3 Relationship between  $\delta D$  and  $\delta^{18}O$  in various water bodies in the SYR Basin during  
 278 different seasons (a) Spring, (b) Summer, (c) Autumn, (d) The contrast between RWL, GWL,  
 279 LMWL and GMWL throughout the sampling period.

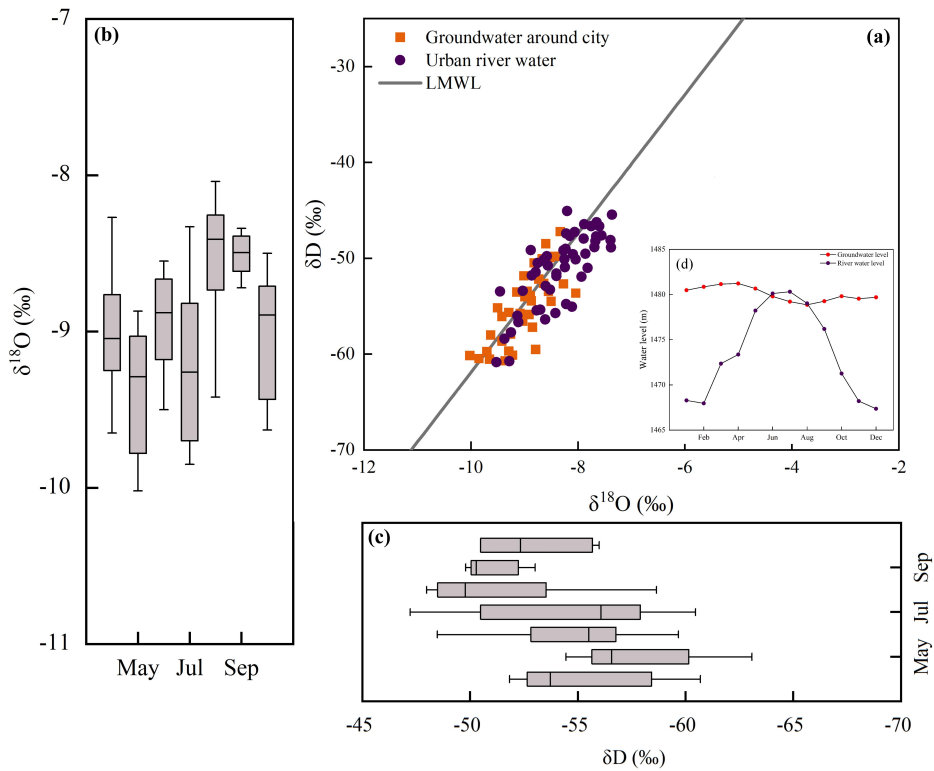
280 Isotopic analysis of groundwater samples reveals a range of  $\delta D$  and  $\delta^{18}O$  values  
 281 spanning from  $-50.7\text{‰}$  to  $-71.9\text{‰}$  and from  $-7.23\text{‰}$  to  $-10.4\text{‰}$ , respectively.  
 282 Moreover, the groundwater samples analyzed in the study displayed a linear  
 283 regression of  $\delta D = 6.3\delta^{18}O - 2.15$  ( $R^2 = 0.86$ ). And it is interesting to note that  
 284 groundwater also shows significant enrichment near the urban landscape dams (Fig.  
 285 2), indicating that groundwater is also affected by evapotranspiration, mainly because  
 286 the Wuwei urban area is in the region of a large alluvial fan in front of the mountains,  
 287 the sand and gravel aquifers are very permeable, and the depth of groundwater burial

288 is shallow, making the groundwater more susceptible to the effects of evaporation.

### 289 **4.3 Impact of urbanization on groundwater**

290 We compared monthly variations in isotopic values of groundwater near the city  
291 with monthly variations in river water from a landscaped dam and found that the  
292 monthly variations in groundwater near the city were closely related to river water  
293 from a landscaped dam. The concentration of groundwater sampling sites near the city  
294 near the sampling sites of the dam water indicates that the groundwater around the  
295 city has similar isotopic signatures to the dam and river water (Fig. 4). This suggests  
296 that groundwater near the city is recharged by river water during the summer months.  
297 In addition, we demonstrated this by comparing the data of the dam river water with  
298 the groundwater level. In addition, a portion of the groundwater sampling sites around  
299 the city are located in the lower right corner of the LMWL, which suggests that the  
300 groundwater around the city may also experience some degree of evaporation.

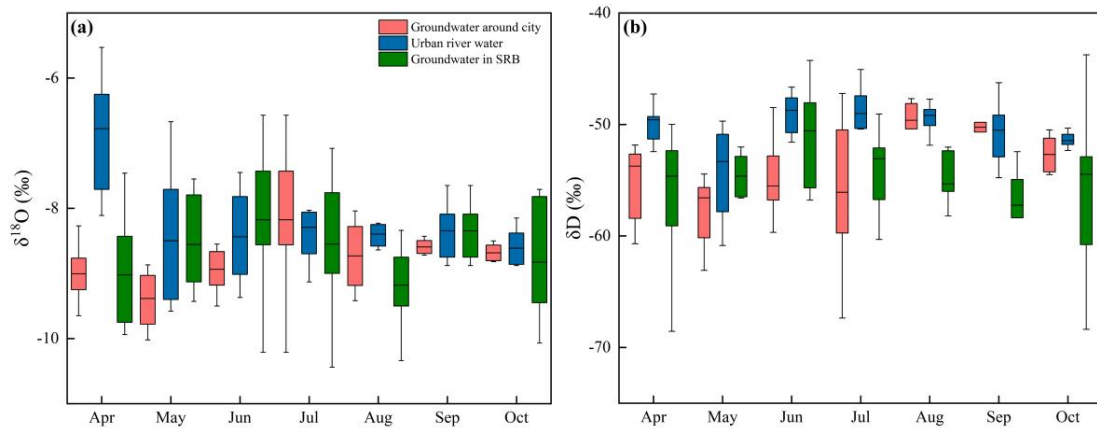




301  
 302 Figure 4 (a) Relationship between  $\delta^{18}\text{O}$  and  $\delta\text{D}$  of groundwater around city and urban river water;  
 303 (b) Monthly variations of  $\delta^{18}\text{O}$  in groundwater around city; (c) Monthly variations of  $\delta\text{D}$  in  
 304 groundwater around city.

305 In addition, we also compared and analyzed the changes of groundwater isotope  
 306 values with those of groundwater around the city in the whole basin, and found that  
 307 there was a close correlation between the changes of groundwater around the city and  
 308 those of the river, while the other groundwater isotope values did not have a strong  
 309 correlation with the river (Fig. 5). In the urban area, the mean values of  $\delta\text{D}$  and  $\delta^{18}\text{O}$   
 310 of the dammed river water were  $-8.26\text{‰}$  and  $-49.88\text{‰}$ , respectively, while the mean  
 311 values of  $\delta\text{D}$  and  $\delta^{18}\text{O}$  of the groundwater around the city were  $-8.44\text{‰}$  and  $-50.36\text{‰}$ ,  
 312 respectively, which indicated that the  $\delta\text{D}$  and  $\delta^{18}\text{O}$  values of the groundwater around  
 313 the city were similar to those of the river water in the dammed city. In addition, the  
 314 isotopic mean values of  $\delta\text{D}$  and  $\delta^{18}\text{O}$  of groundwater throughout the SYR basin were

315 -8.73‰ and -54.78‰, which are significantly different from the isotopic values of  
316 river water in the urban dam.

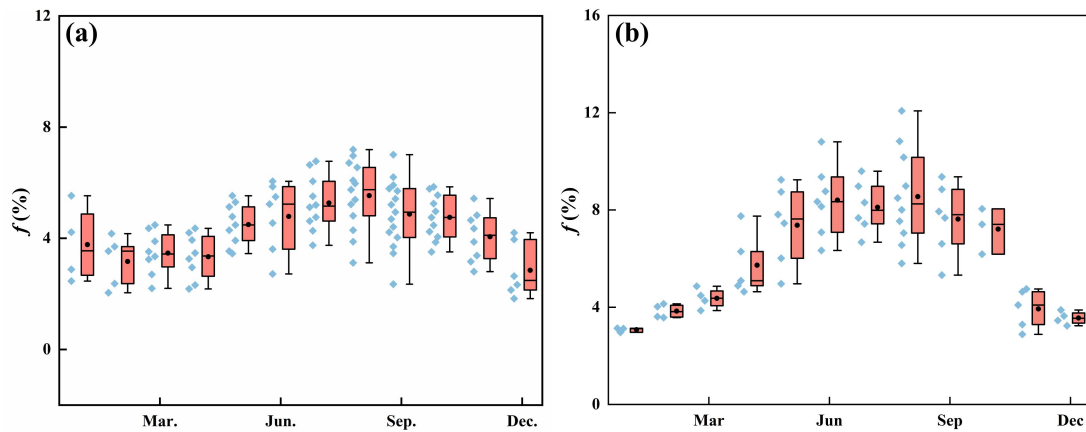


317  
318 Figure 5 (a) Monthly variations of  $\delta^{18}\text{O}$  in urban river water and groundwater around city, (b)  
319 Monthly variations of  $\delta\text{D}$  in urban river water and groundwater around city.

#### 320 **4.4 Temporal and spatial variation of surface water evaporation losses in the** 321 **urban area of Wuwei**

322 In addition to being an essential part of the hydrological cycle, evaporation is  
323 widely recognized as one of the most significant factors driving climate change in  
324 semi-arid regions and in telluric ecosystems (Gibson et al., 2002; Gibson and Edwards,  
325 2002). An obviously spatial and temporal fluctuation can be seen in the amount of  
326 surface water that is lost to evaporation in the upper mountain area as well as the  
327 intermediate urban area of the SYR basin (Fig. 6). Analyzed from a time-varying  
328 perspective, there is significant seasonal variation in surface water evaporation losses  
329 both in the upstream mountainous region and the midstream urban area of Wuwei,  
330 with the highest rates occurring during summer and the lowest during winter (Fig.6).  
331 Additionally, a spatial comparison reveals that surface water evaporation losses in the  
332 midstream urban area of Wuwei are significantly greater than those in the upstream

333 mountainous area.



334

335 Figure 6 Evaporation losses from surface water in different areas of the SYR (a) Upper reaches

336 mountainous area, (b) Middle reaches urban areas.

337 Differences contributing to evaporation losses from the river in the upstream and

338 midstream urban areas can be explained mainly by the landscape characteristics of the

339 basin. In the upstream of the Shiyang River, higher vegetation cover and atmospheric

340 humidity in the mountainous areas result in weaker evaporation losses, while the

341 midstream are dominated by urban land, and urban landscapes increase the watershed

342 area and slow down the river, exacerbating evaporation losses from the river.

## 343 5 Discussion

### 344 5.1 Effects of Urbanization on the Rainfall-Runoff Process

345 Fig. 7 depicts the regression model of rainfall events in the SYR Basin,

346 represented by a sine wave, and the fitting of surface water  $\delta^{18}\text{O}$  across the research

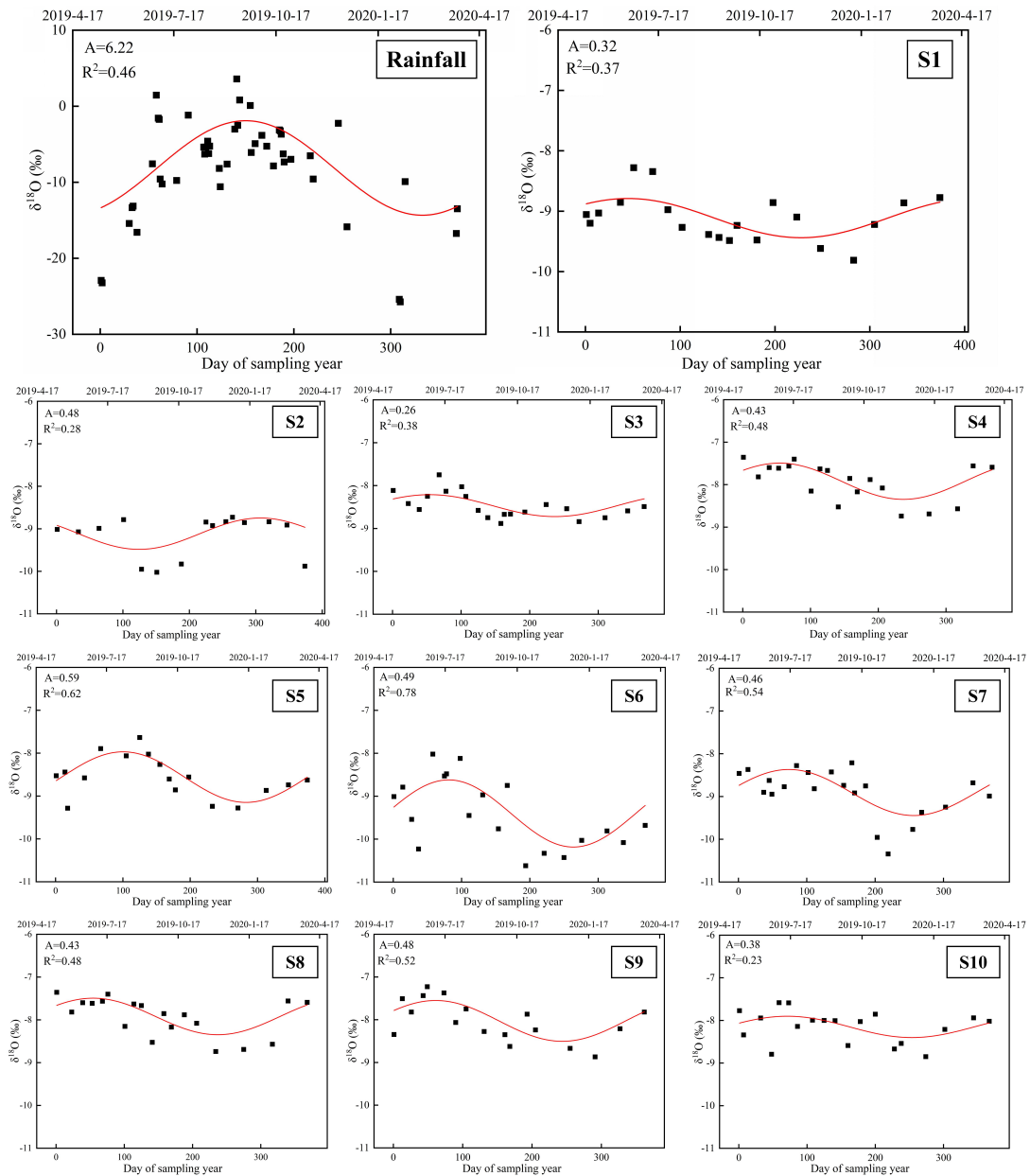
347 season. The  $\delta^{18}\text{O}$  levels of precipitation reported in the SYR Basin have an excellent

348 regularity ( $R^2=0.46$ ) and a seasonal patterns trend that effectively depicts the nfluence

349 of the monsoon climate on the local environment (Zhu et al., 2019). Seasonal

350 variations are seen in the generally steady  $\delta^{18}\text{O}$  and  $\delta^{18}\text{O}$  values of the upstream water.

351 These results indicate that the predominant component of the river water is the  
352 baseflow resulting from recent precipitation runoff. Throughout the duration of the  
353 study, the majority of the lowest  $\delta^{18}\text{O}$  values in the 10 surface water sample points  
354 were recorded during the winter, whilst the highest values were recorded during the  
355 summer. These trends coincide with both the temporal variation of precipitation  
356 isotopes in the SYR Basin, indicating that precipitation input is the underlying cause  
357 of isotope changes in river water. Nevertheless, variations in the isotopes of river  
358 water differ in range across various regions within the SYR Basin, with significant  
359 variation in the degree of fit for the regression curve. The fitting degree of surface  
360 water in the upper and lower reaches is relatively low ( $R^2=0.37$ ,  $R^2=0.28$ ,  $R^2=0.23$ ),  
361 implying limited seasonal isotopic variability in these regions. The midstream surface  
362 water exhibits a notably higher degree of conformity as compared to its upstream and  
363 downstream counterparts ( $R^2=0.38$ ,  $R^2=0.48$ ,  $R^2=0.62$ ,  $R^2=0.78$ ,  $R^2=0.54$ ,  $R^2=0.48$ ,  
364  $R^2=0.52$ ). Moreover, the isotopic composition of surface water throughout this area  
365 exhibits notable cyclic variations.



366

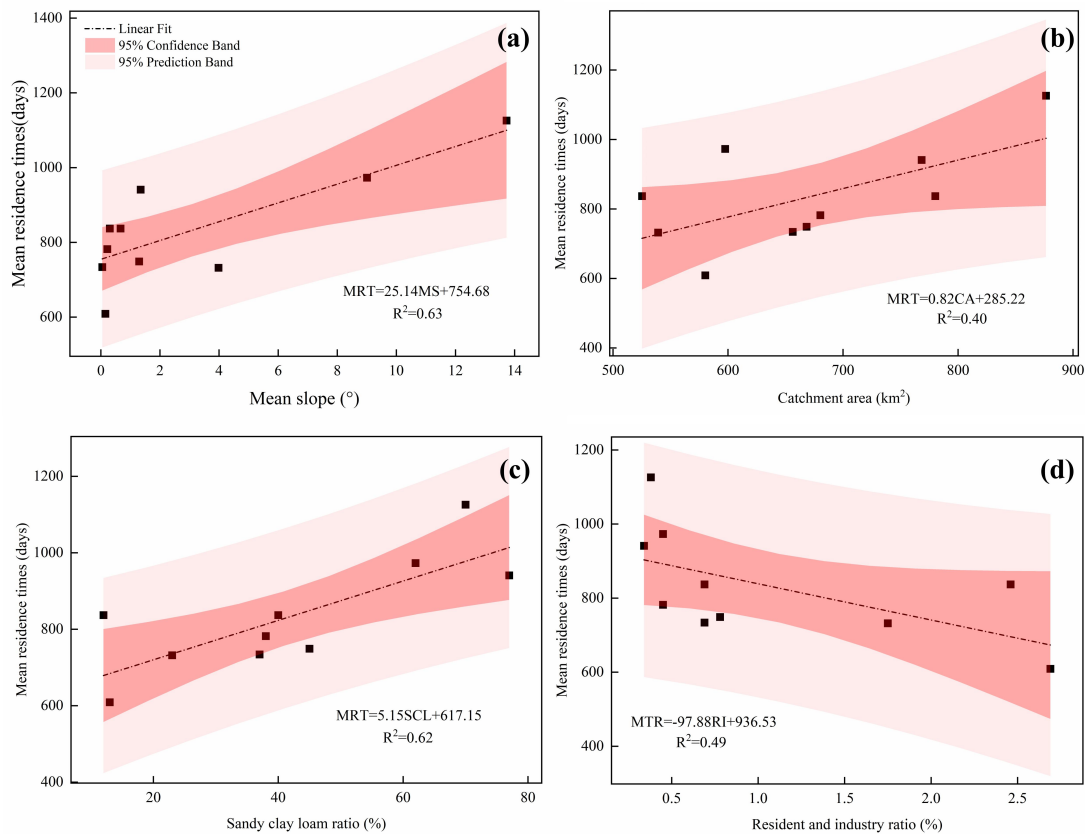
367 Figure 7 Fits the annual regression model of  $\delta^{18}\text{O}$  in SYR Basin precipitation and river water (time:  
 368 2019/4/17—2020/4/23; S1-S10 are surface water sampling points).

369 The reasons for differences in isotope periodicity in different regions may be  
 370 attributed to local water management systems, topographic features and urban  
 371 development. At points S1, S2, and S10, the correlation of model simulations was low,  
 372 which could be attributed to the presence of Xiyang Reservoir in the upstream as well  
 373 as Hongyashan Reservoir in the downstream (Sang et al., 2023), where seasonal

374 variations in the isotope values of the river water are interfered by the reservoir  
375 dispatching activities. At points S3 to S5, the correlation of the model simulation is  
376 higher, which is because in the middle reaches of the SYR basin, the expansion of  
377 urban built-up areas leads to a significant increase in surface runoff during the rainy  
378 season, and according to the land use data, the land area of the towns in Wuwei City  
379 has continued to increase by 134.38 km<sup>2</sup> from 2010 to 2018, resulting in the surface  
380 water showing a cyclical trend comparable to that of the precipitation. Since the 1950s,  
381 in order to better utilize water resources, 13 small and medium-sized reservoirs with a  
382 total storage capacity of 900,000 m<sup>3</sup> were constructed during this period (Ma et al.,  
383 2010), increasing the proportion of rainfall in the runoff constituents as a result of The  
384 correlation of the model simulation is at a high level at points S6~S9, where, in  
385 contrast to the high-elevation areas in the upper reaches, the terrain in the middle and  
386 lower reaches of the SYR basin is relatively flat, mainly with cultivated land and  
387 deserts, and is less disturbed by human activities (Sun et al., 2021), which further  
388 reflects the responsiveness to recent precipitation inputs.

389         The Dunnett's test revealed a significant difference ( $P < 0.05$ ) between the MRT  
390 of the river and the annual magnitude of  $\delta^{18}\text{O}$  of the river. We further investigated the  
391 relationship between the estimated mean residence time and basin landscape features  
392 such as topography (Fig. 8). Using the digital elevation model (DEM) to calculate the  
393 mean slope of the SYR basin, we found that the mean residence time was also  
394 strongly correlated with the mean basin slope ( $R^2 = 0.63$ ), and that the upper reaches  
395 of the Shiyang River basin are mainly high-elevation mountainous areas, where the

396 topography is sloped, but where the vegetation cover is high and dominated by alpine  
 397 meadows, subalpine scrub and Qinghai spruce (Zhang et al. 2023), the greater slope  
 398 leads to a higher gravitational potential, which tends to result in a negative correlation  
 399 with mean residence time (McGuire et al., 2005), which also contributes to the  
 400 potentially higher MRT values in the upstream mountains. In our study, catchment  
 401 area (CA) had a low correlation with MRT ( $R^2 = 0.40$ ), and a weak relationship  
 402 between catchment area and MRT has been observed in other studies (McGlynn et al.,  
 403 2003; McGuire et al., 2005).



404  
 405 Figure 8 Correlation between mean slope of the basin (a), catchment area (b), sand clay loam ratio  
 406 (c), ratio of residential and industrial areas to total basin area (d) and MRT.

407 Soil is an important component of basin hydrology, and the physical properties  
 408 of soil, such as water-holding capacity and pore space distribution, have an important

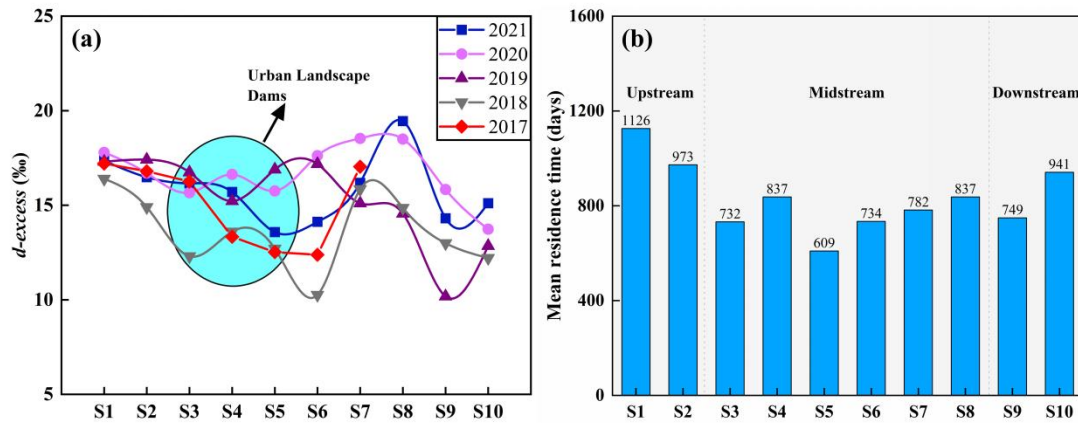
409 influence on the response to precipitation in the basin and the sand-clay-loam soil  
410 ratio is used here to investigate the possible relationship with MRT. The results  
411 showed that the content of sand clay loam ratio showed a strong positive correlation  
412 with MRT ( $R^2=0.62$ ). Wuwei City is located in the pre-mountain flood-fan belt, and  
413 the soil is dominated by sandy soil (Zhang et al., 2023), which is loose in texture, has  
414 good permeability and good water retention properties, and is mainly used for  
415 agricultural cultivation. Its good permeability increases the vertical movement of  
416 water and the length of flow paths, leading to a longer MRT. There is a strong  
417 negative correlation between the MRT and the ratios of resident and industrial areas  
418 (RI) ( $R^2=0.49$ ), which also indicates that as urbanization progresses, with the increase  
419 of urban land, this undoubtedly leads to a significant shortening of the MRT. However,  
420 the MRT in the mid-river urban area is not much shorter as compared to the  
421 downstream, which may be attributed to the fact that the mid-river The large number  
422 of landscape dams constructed in the urban areas, currently 51 urban landscape dams  
423 have been built in the peri-urban areas of Wuwei City, and the considerable number of  
424 landscape dams may have counteracted the impact of the urban land use, resulting in a  
425 lengthening of the MRT in the middle reaches as well.

## 426 **5.2 Effects of Water Conservancy Projects in Urban Areas on Isotope Dynamics**

427 Recent studies have suggested that the development of dam-reservoir systems  
428 may result in river fragmentation and modifications in flow regimes in terms of their  
429 volume, frequency, and duration (Négrel et al., 2016; Murgulet et al., 2016; Peñas and  
430 Barquín, 2019; Maavara et al., 2020). Furthermore, chemical-containing nutrient



431 migration, such as phosphorus, may occur during sediment movement, resulting in  
432 widespread eutrophication problems (Yang et al., 2007; Duan et al., 2019). As of 2019,  
433 a total of 51 urban landscape dams, primarily consisting of artificial landscape  
434 waterfalls and rubber dams, have been constructed in and around Wuwei city (Zhu et  
435 al., 2021). In the metropolitan coast of Wuwei, many landscape dams have led to  
436 isotopic enrichment in surface water. This damping effect has been observed in  
437 numerous dammed rivers across the globe, including the Rio Grande in the  
438 southwestern United States (Vitvar et al., 2007) and the Ebro River in Spain (Négrel  
439 et al., 2016), as evidenced by isotopic tracers. In the metropolitan coast of Wuwei, a  
440 number of landscape dams have led to the enrichment of isotopic tracers in the surface  
441 water. The results indicate that the  $\delta D$  and  $\delta^{18}O$  levels of the surface water at the  
442 outflow of Wuwei City are greater than those at the inflow (Fig. 2). Moreover, the  
443 influence of evaporation on isotopic composition should not be overlooked, as it can  
444 lead to a decrease in *d-excess* values (Peng et al., 2012). Consistent with previous  
445 studies (Wang et al., 2019), we observed that the *d-excess* of influent water was higher  
446 than that of urban river water. This observation further supports the accumulation of  
447 heavy H-O isotopes in the surface waters of the dam areas, as shown in Fig. 6a. In  
448 contrast, due to the confluence of tributaries prior to the S7 sampling point, the river  
449 water has lower isotopic values, resulting in elevated *d-excess* values between S6 and  
450 S8.



451

452 Figure 9 (a) The longitudinal variation of the surface water *d-excess* of the SYR, (b) The

453 longitudinal variation of the surface water MRT of the SYR.

### 454 5.3 Effects of Urbanization on the Water Cycle of basins

455 Localized microclimates in urban areas allow for changes in precipitation and

456 evapotranspiration processes, while urbanization alters the pristine subsurface,

457 complicating water cycle processes in the basin (Jacobson, 2011; Westra et al., 2014;

458 Oudin et al., 2018). In terms of the impact on runoff, it is mainly reflected in the

459 increase of surface impermeability due to urbanization, the land use area of Wuwei

460 urban land increased by about 134.38 km<sup>2</sup> from 2010 to 2018, which greatly

461 weakened the infiltration process in urban areas, and the rainfall runoff process

462 simulated by sinusoidal cyclic regression method showed that there were significant

463 differences in the river metro in different parts of the Shiyang River Basin, and that

464 the middle reaches of the river had the highest degree of urbanization, and the time of

465 the metro was the shortest, which further increases the contribution of rainfall to

466 runoff. Regarding the effect of urbanization on evapotranspiration, a large number of

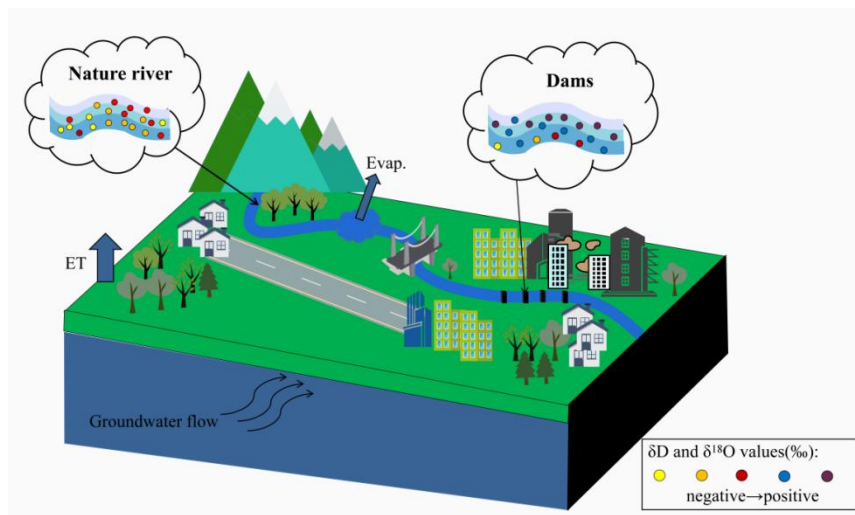
467 dams were constructed on the Shiyang River and flowed through the urban area of

468 Wuwei, causing significant evapotranspiration losses, in addition, these landscape

469 dams also led to hydrogen and oxygen isotope enrichment (Fig. 10), and the  
470 numerous reservoirs that were constructed for the construction and development of  
471 the city (Ma et al., 2010), and these reservoirs also contributed to a significant  
472 evapotranspiration loss effect, which has been previously confirmed in our study was  
473 also confirmed (Sang et al., 2023). On the other hand, our study found that the  
474 isotopic compositions and trends of urban nearshore groundwater were similar to  
475 those of surface water, which suggests that there is a close correlation between urban  
476 nearshore groundwater and river water, and that the difference in water levels between  
477 river water and groundwater may be the main reason for river recharge of urban  
478 nearshore groundwater (Fig. 4). In the rainy season, the river level gradually rises,  
479 which decreases the difference between the water levels of urban nearshore  
480 groundwater and river water, and the river water recharges the groundwater, and in the  
481 dry season, the river level decreases, and the urban nearshore groundwater, which is  
482 buried at a shallow depth, in turn recharges the river.

483 In addition, the growth of urbanization has had a dramatic impact on the water  
484 environment in cities, where water problems occur frequently (Giri and Qiu, 2016;  
485 Ma et al., 2022). Urbanization has increased impervious surfaces such as parking lots,  
486 rooftops, roads, and sidewalks, leading to increased runoff, which creates additional  
487 pathways for pollutants to be transported from landscapes to water bodies (Ren et al.,  
488 2014; Wilson and Weng, 2010; Nolan et al., 2023). On the other hand, agricultural  
489 activities have increased some of the fertilizers, pesticides, herbicides and dairy  
490 manure in the farmland into the nearest water bodies, which can directly and

491 indirectly affect will reduce water quality (Yu et al., 2013). The Shiyang River Basin  
492 in the Northwest Arid Zone is an inland river basin with the highest development  
493 intensity and the sharpest conflict between water supply and demand in the region.  
494 The Liangzhou district in the central part of the Shiyang River basin is the most  
495 densely populated artificial oasis with the largest scale of water demand in the entire  
496 basin. Our previous study found that direct discharge of industrial and community  
497 domestic wastewater into the river led to deterioration of surface water quality around  
498 the Shiyang River basin (Ma et al., 2021). In addition agricultural activities have less  
499 impact on the upper reaches of the Shiyang River and relatively more impact on the  
500 middle and lower reaches , and the application of nitrogen-based fertilizers during  
501 agricultural cultivation is the main cause of high  $\text{NH}_4^+$  and  $\text{NO}_3^-$  concentrations in the  
502 area (Ma et al., 2021), which may also lead to increased salinity and accelerated  
503 eutrophication of the river, threatening the safety of the basin's water environment.  
504 Overall, human activities (urbanization) may alter the water cycle processes inherent  
505 in inland river basins, and the implications of such changes need to be further  
506 explored.



507

508 Figure 10 Schematic diagram of the effect of urbanization on river isotope dynamics.

## 509 **6 Conclusions**

510 In this study, we investigated the hydrometeorological and isotopic data of the  
511 Shiyang River Basin from 2017 to 2021, and our investigations showed that  
512 urbanization had a significant impact on the water cycle of the basin. The results  
513 showed that the isotopic values of the river water showed a significant enrichment  
514 from upstream to downstream, but facilities such as landscape dams and reservoirs in  
515 the urban area significantly altered this natural pattern, and the isotopic values of the  
516 river water in the urban area ( $\delta D = -48.31\text{‰}$ ;  $\delta^{18}O = -7.49\text{‰}$ ) were higher than those of  
517 the natural river water ( $\delta D = -55.77\text{‰}$ ;  $\delta^{18}O = -8.98\text{‰}$ ), and landscape dams aggravated  
518 the evaporation losses of river water, due to the increase of urban land area, which  
519 accelerated the rainfall-runoff conversion process, the residence time of surface water  
520 in different regions of the Shiyang River Basin had obvious differences, and the MRT  
521 from the upstream to the downstream showed a fluctuating downward process, which  
522 was shortened from 1,126 days in the upstream to 941 days in the downstream, and  
523 the MRT was mainly controlled by the basin's landscape features. In addition, there  
524 was a strong relationship between the isotopic composition of the reservoir and the  
525 surrounding groundwater. Overall, urbanization has a profound impact on the  
526 hydrological system of the basin, and the results of this study can provide some  
527 references for future research on urbanization and the water cycle, and improve our  
528 understanding of the hydrological processes of basin in arid zones.

## 529 **Acknowledgements**

530 This research was financially supported by the National Natural Science  
531 Foundation of China (41971036, 41867030).

### 532 **Author contributions statement**

533 Rui Li: Writing-Original draft preparation; Guofeng Zhu: Writing-Reviewing and  
534 Editing; Siyu Lu: Methodology; Liyuan Sang and Gaojia Meng: Data processing and  
535 Experiment; Longhu Chen and Yinying Jiao: Methodology and visualization;  
536 Qinqin Wang : Visualization;

### 537 **Data availability Statement**

538 The isotopic data that support the findings of this study are openly available in  
539 Zhu, Guofeng (2022), “Stable water isotope monitoring network of different water  
540 bodies in SYR Basin, a typical arid river in China”, Mendeley Data, V1, doi:  
541 10.17632/vhm44t74sy.1. The source of soil data comes from the Harmonized World  
542 Soil Database (HWSD) constructed by the Food and Agriculture Organization of the  
543 United Nations (FAO) and the International Institute for Applied Systems (IIASA) on  
544 2009. The land-use and land-cover change data of the Shiyang River Basin were  
545 obtained from Chinese Academy of Sciences, the data centre of resources and  
546 environmental science (<http://www.resdc.cn>).

### 547 **Competing Interests**

548 We undersigned declare that this manuscript entitled “Effects of Urbanization on  
549 the water cycle in the SYR Basin: Based on stable isotope method” is original, has not  
550 been published before and is not currently being considered for publication elsewhere.

551 The authors declare that they have no known competing financial interests or

552 personal relationships that could have appeared to influence the work reported in this  
553 paper.

#### 554 **Reference**

555 Anderson, B. J., Slater, L. J., Dadson, S. J., Blum, A. G., and Prosdocimi, I.:  
556 Statistical Attribution of the Influence of Urban and Tree Cover Change on  
557 Streamflow: A Comparison of Large Sample Statistical Approaches, *Water*  
558 *Resources Research*, 58, e2021WR030742,  
559 <https://doi.org/10.1029/2021WR030742>, 2022.

560 Asano, Y., Uchida, T., and Ohte, N.: Residence times and flow paths of water in steep  
561 unchannelled catchments, Tanakami, Japan, *Journal of Hydrology*, 261, 173–192,  
562 [https://doi.org/10.1016/S0022-1694\(02\)00005-7](https://doi.org/10.1016/S0022-1694(02)00005-7), 2002.

563 Baker, A.: Land Use and Water Quality, in: *Encyclopedia of Hydrological Sciences*,  
564 edited by: Anderson, M. G. and McDonnell, J. J., John Wiley & Sons, Ltd,  
565 Chichester, UK, hsa195, <https://doi.org/10.1002/0470848944.hsa195>, 2005.

566 Bhaskar, A. S. and Welty, C.: Analysis of subsurface storage and streamflow  
567 generation in urban basins, *Water Resour. Res.*, 51, 1493–1513,  
568 <https://doi.org/10.1002/2014WR015607>, 2015.

569 Blum, A. G., Ferraro, P. J., Archfield, S. A., and Ryberg, K. R.: Causal Effect of  
570 Impervious Cover on Annual Flood Magnitude for the United States,  
571 *Geophysical Research Letters*, 47, e2019GL086480,  
572 <https://doi.org/10.1029/2019GL086480>, 2020.

573 Bruwier, M., Maravat, C., Mustafa, A., Teller, J., Piroton, M., Erpicum, S.,  
574 Archambeau, P., and Dewals, B.: Influence of urban forms on surface flow in

575 urban pluvial flooding, *Journal of Hydrology*, 582, 124493,  
576 <https://doi.org/10.1016/j.jhydrol.2019.124493>, 2020.

577 Burian, S. J. and Shepherd, J. M.: Effect of urbanization on the diurnal rainfall pattern  
578 in Houston, *Hydrol. Process.*, 19, 1089–1103, <https://doi.org/10.1002/hyp.5647>,  
579 2005.

580 Caldwell, P. V., Sun, G., McNulty, S. G., Cohen, E. C., and Moore Myers, J. A.:  
581 Impacts of impervious cover, water withdrawals, and climate change on river  
582 flows in the conterminous US, *Hydrol. Earth Syst. Sci.*, 16, 2839–2857,  
583 <https://doi.org/10.5194/hess-16-2839-2012>, 2012.

584 Chen, G., Li, X., Liu, X., Chen, Y., Liang, X., Leng, J., Xu, X., Liao, W., Qiu, Y., Wu,  
585 Q., and Huang, K.: Global projections of future urban land expansion under  
586 shared socioeconomic pathways, *Nat Commun*, 11, 537,  
587 <https://doi.org/10.1038/s41467-020-14386-x>, 2020.

588 Dansgaard, W.: Stable isotopes in precipitation, *Tellus*, 16, 436–468,  
589 <https://doi.org/10.1111/j.2153-3490.1964.tb00181.x>, 1964.

590 De Niel, J. and Willems, P.: Climate or land cover variations: what is driving observed  
591 changes in river peak flows? A data-based attribution study, *Hydrol. Earth Syst.*  
592 *Sci.*, 23, 871–882, <https://doi.org/10.5194/hess-23-871-2019>, 2019.

593 Deng, K., Yang, S., Lian, E., Li, C., Yang, C., and Wei, H.: Three Gorges Dam alters  
594 the Changjiang (Yangtze) river water cycle in the dry seasons: Evidence from  
595 H-O isotopes, *Science of The Total Environment*, 562, 89–97,  
596 <https://doi.org/10.1016/j.scitotenv.2016.03.213>, 2016.



597 Duan, W., Hanasaki, N., Shiogama, H., Chen, Y., Zou, S., Nover, D., Zhou, B., and  
598 Wang, Y.: Evaluation and Future Projection of Chinese Precipitation Extremes  
599 Using Large Ensemble High-Resolution Climate Simulations, *Journal of Climate*,  
600 32, 2169–2183, <https://doi.org/10.1175/JCLI-D-18-0465.1>, 2019.

601 Fekete, B. M., Gibson, J. J., Aggarwal, P., and Vörösmarty, C. J.: Application of  
602 isotope tracers in continental scale hydrological modeling, *Journal of Hydrology*,  
603 330, 444–456, <https://doi.org/10.1016/j.jhydrol.2006.04.029>, 2006.

604 Flörke, M., Schneider, C., and McDonald, R. I.: Water competition between cities and  
605 agriculture driven by climate change and urban growth, *Nat Sustain*, 1, 51–58,  
606 <https://doi.org/10.1038/s41893-017-0006-8>, 2018.

607 Förstel, H. and Hützen, H.: Oxygen isotope ratios in German groundwater, *Nature*,  
608 304, 614–616, <https://doi.org/10.1038/304614a0>, 1983.

609 Fu, X., Yang, X., and Sun, X.: Spatial and Diurnal Variations of Summer Hourly  
610 Rainfall Over Three Super City Clusters in Eastern China and Their Possible  
611 Link to the Urbanization, *JGR Atmospheres*, 124, 5445–5462,  
612 <https://doi.org/10.1029/2019JD030474>, 2019.

613 Gammons, C. H., Poulson, S. R., Pellicori, D. A., Reed, P. J., Roesler, A. J., and  
614 Petrescu, E. M.: The hydrogen and oxygen isotopic composition of precipitation,  
615 evaporated mine water, and river water in Montana, USA, *Journal of Hydrology*,  
616 328, 319–330, <https://doi.org/10.1016/j.jhydrol.2005.12.005>, 2006.

617 Gessner, M. O., Hinkelmann, R., Nützmann, G., Jekel, M., Singer, G., Lewandowski,  
618 J., Nehls, T., and Barjenbruch, M.: Urban water interfaces, *Journal of Hydrology*,  
619 514, 226–232, <https://doi.org/10.1016/j.jhydrol.2014.04.021>, 2014.

620 Gibson, J. J., Edwards, T. W. D., Birks, S. J., St Amour, N. A., Buhay, W. M.,  
621 McEachern, P., Wolfe, B. B., and Peters, D. L.: Progress in isotope tracer  
622 hydrology in Canada, *Hydrol. Process.*, 19, 303–327,  
623 <https://doi.org/10.1002/hyp.5766>, 2005.

624 Gibson, J. J. and Edwards, T. W. D.: Regional water balance trends and  
625 evaporation-transpiration partitioning from a stable isotope survey of lakes in  
626 northern Canada: REGIONAL WATER BALANCE USING STABLE  
627 ISOTOPES, *Global Biogeochem. Cycles*, 16, 10-1-10–14,  
628 <https://doi.org/10.1029/2001GB001839>, 2002.

629 Gibson, J. J., Prepas, E. E., and McEachern, P.: Quantitative comparison of lake  
630 throughflow, residency, and catchment runoff using stable isotopes: modelling  
631 and results from a regional survey of Boreal lakes, *Journal of Hydrology*, 2002.

632 Gillefalk, M., Tetzlaff, D., Hinkelmann, R., Kuhlemann, L.-M., Smith, A., Meier, F.,  
633 Maneta, M. P., and Soulsby, C.: Quantifying the effects of urban green space on  
634 water partitioning and ages using an isotope-based ecohydrological model,  
635 *Hydrol. Earth Syst. Sci.*, 25, 3635–3652,  
636 <https://doi.org/10.5194/hess-25-3635-2021>, 2021.

637 Giri, S. and Qiu, Z.: Understanding the relationship of land uses and water quality in  
638 Twenty First Century: A review, *Journal of Environmental Management*, 173,  
639 41–48, <https://doi.org/10.1016/j.jenvman.2016.02.029>, 2016.

640 Grimm, N. B., Faeth, S. H., Golubiewski, N. E., Redman, C. L., Wu, J., Bai, X., and  
641 Briggs, J. M.: Global Change and the Ecology of Cities, *Science*, 319, 756–760,  
642 <https://doi.org/10.1126/science.1150195>, 2008.

643 Guan, M., Sillanpää, N., and Koivusalo, H.: Storm runoff response to rainfall pattern,  
644 magnitude and urbanization in a developing urban catchment: Storm Runoff  
645 Response to Rainfall Pattern, Magnitude and Urbanization, *Hydrol. Process.*,  
646 n/a-n/a, <https://doi.org/10.1002/hyp.10624>, 2015.

647 Hamilton, S. K., Bunn, S. E., Thoms, M. C., and Marshall, J. C.: Persistence of  
648 aquatic refugia between flow pulses in a dryland river system(Cooper Creek,  
649 Australia), *Limnol. Oceanogr.*, 50, 743–754,  
650 <https://doi.org/10.4319/lo.2005.50.3.0743>, 2005.

651 Han, S., Slater, L., Wilby, R. L., and Faulkner, D.: Contribution of urbanisation to  
652 non-stationary river flow in the UK, *Journal of Hydrology*, 613, 128417,  
653 <https://doi.org/10.1016/j.jhydrol.2022.128417>, 2022.

654 Jacobson, C. R.: Identification and quantification of the hydrological impacts of  
655 imperviousness in urban catchments: A review, *Journal of Environmental*  
656 *Management*, 92, 1438–1448, <https://doi.org/10.1016/j.jenvman.2011.01.018>,  
657 2011.

658 Liu, J., Shen, Z., and Chen, L.: Assessing how spatial variations of land use pattern  
659 affect water quality across a typical urbanized basin in Beijing, China,  
660 *Landscape and Urban Planning*, 176, 51–63,  
661 <https://doi.org/10.1016/j.landurbplan.2018.04.006>, 2018.

662 Ma, H., Zhu, G., Zhang, Y., Sang, L., Wan, Q., Zhang, Z., Xu, Y., and Qiu, D.: Ion  
663 migration process and influencing factors in inland river basin of arid area in  
664 China: a case study of Shiyang River Basin, *Environ Sci Pollut Res*, 28,  
665 56305–56318, <https://doi.org/10.1007/s11356-021-14484-3>, 2021.

666 Ma, J., Pan, F., Chen, L., Edmunds, W. M., Ding, Z., He, J., Zhou, K., and Huang, T.:  
667 Isotopic and geochemical evidence of recharge sources and water quality in the  
668 Quaternary aquifer beneath Jinchang city, NW China, *Applied Geochemistry*, 25,  
669 996–1007, <https://doi.org/10.1016/j.apgeochem.2010.04.006>, 2010.

670 Ma, X., Li, N., Yang, H., and Li, Y.: Exploring the relationship between urbanization  
671 and water environment based on coupling analysis in Nanjing, East China,  
672 *Environ Sci Pollut Res*, 29, 4654–4667,  
673 <https://doi.org/10.1007/s11356-021-15161-1>, 2022.

674 Maavara, T., Chen, Q., Van Meter, K., Brown, L. E., Zhang, J., Ni, J., and Zarfl, C.:  
675 River dam impacts on biogeochemical cycling, *Nat Rev Earth Environ*, 1,  
676 103–116, <https://doi.org/10.1038/s43017-019-0019-0>, 2020.

677 Małoszewski, P., Rauert, W., Stichler, W., and Herrmann, A.: Application of flow  
678 models in an alpine catchment area using tritium and deuterium data, *Journal of*  
679 *Hydrology*, 66, 319–330, [https://doi.org/10.1016/0022-1694\(83\)90193-2](https://doi.org/10.1016/0022-1694(83)90193-2), 1983.

680 Martin, K. L., Hwang, T., Vose, J. M., Coulston, J. W., Wear, D. N., Miles, B., and  
681 Band, L. E.: basin impacts of climate and land use changes depend on magnitude  
682 and land use context, *Ecohydrology*, 10, e1870, <https://doi.org/10.1002/eco.1870>,  
683 2017.

684 McDonough, L. K., Santos, I. R., Andersen, M. S., O'Carroll, D. M., Rutledge, H.,  
685 Meredith, K., Oudone, P., Bridgeman, J., Goody, D. C., Sorensen, J. P. R.,  
686 Lapworth, D. J., MacDonald, A. M., Ward, J., and Baker, A.: Changes in global  
687 groundwater organic carbon driven by climate change and urbanization, *Nat*  
688 *Commun*, 11, 1279, <https://doi.org/10.1038/s41467-020-14946-1>, 2020.

689 McGlynn, B., McDonnell, J., Stewart, M., and Seibert, J.: On the relationships  
690 between catchment scale and streamwater mean residence time, *Hydrol. Process.*,  
691 17, 175–181, <https://doi.org/10.1002/hyp.5085>, 2003.

692 McGuire, K. J., McDonnell, J. J., Weiler, M., Kendall, C., McGlynn, B. L., Welker, J.  
693 M., and Seibert, J.: The role of topography on catchment-scale water residence  
694 time: CATCHMENT-SCALE WATER RESIDENCE TIME, *Water Resour. Res.*,  
695 41, <https://doi.org/10.1029/2004WR003657>, 2005.

696 Murgulet, D., Murgulet, V., Spalt, N., Douglas, A., and Hay, R. G.: Impact of  
697 hydrological alterations on river-groundwater exchange and water quality in a  
698 semi-arid area: Nueces River, Texas, *Science of The Total Environment*, 572,  
699 595–607, <https://doi.org/10.1016/j.scitotenv.2016.07.198>, 2016.

700 Négrel, P., Petelet-Giraud, E., and Millot, R.: Tracing water cycle in regulated basin  
701 using stable  $\delta^{18}\text{O}$ – $\delta^2\text{H}$  isotopes: The Ebro river basin (Spain), *Chemical Geology*,  
702 422, 71–81, <https://doi.org/10.1016/j.chemgeo.2015.12.009>, 2016.

703 Nolan, T. M., Reynolds, L. J., Sala-Comorera, L., Martin, N. A., Stephens, J. H.,  
704 O'Hare, G. M. P., O'Sullivan, J. J., and Meijer, W. G.: Land use as a critical  
705 determinant of faecal and antimicrobial resistance gene pollution in riverine  
706 systems, *Science of The Total Environment*, 871, 162052,  
707 <https://doi.org/10.1016/j.scitotenv.2023.162052>, 2023.

708 Oudin, L., Salavati, B., Furusho-Percot, C., Ribstein, P., and Saadi, M.: Hydrological  
709 impacts of urbanization at the catchment scale, *Journal of Hydrology*, 559,  
710 774–786, <https://doi.org/10.1016/j.jhydrol.2018.02.064>, 2018.

711 Peñas, F. J. and Barquín, J.: Assessment of large-scale patterns of hydrological  
712 alteration caused by dams, *Journal of Hydrology*, 572, 706–718,  
713 <https://doi.org/10.1016/j.jhydrol.2019.03.056>, 2019.

714 Peng, T.-R., Huang, C.-C., Wang, C.-H., Liu, T.-K., Lu, W.-C., and Chen, K.-Y.:  
715 Using oxygen, hydrogen, and tritium isotopes to assess pond water's contribution  
716 to groundwater and local precipitation in the pediment tableland areas of  
717 northwestern Taiwan, *Journal of Hydrology*, 450–451, 105–116,  
718 <https://doi.org/10.1016/j.jhydrol.2012.05.021>, 2012.

719 Pickett, S. T. A., Cadenasso, M. L., Grove, J. M., Boone, C. G., Groffman, P. M.,  
720 Irwin, E., Kaushal, S. S., Marshall, V., McGrath, B. P., Nilon, C. H., Pouyat, R.  
721 V., Szlavecz, K., Troy, A., and Warren, P.: Urban ecological systems: Scientific

722 foundations and a decade of progress, *Journal of Environmental Management*, 92,  
723 331–362, <https://doi.org/10.1016/j.jenvman.2010.08.022>, 2011.

724 Qian, H., Dou, Y., Li, X.J., Yang, B.C., and Zhao, Z.H.: Changes of  $\delta^{18}\text{O}$  and  $\delta\text{D}$   
725 along Dousitu River and its indication of river water evaporation. *Hydrogeol.*  
726 *Eng. Geol.* 34 (1), 107–112,  
727 <https://doi.org/10.16030/j.cnki.issn.1000-3665.2007.01.024,2007>.

728 Ren, L., Cui, E., and Sun, H.: Temporal and spatial variations in the relationship  
729 between urbanization and water quality, *Environ Sci Pollut Res*, 21,  
730 13646–13655, <https://doi.org/10.1007/s11356-014-3242-8>, 2014.

731 Rodgers, P., Soulsby, C., Waldron, S., and Tetzlaff, D.: Using stable isotope tracers to  
732 assess hydrological flow paths, residence times and landscape influences in a  
733 nested mesoscale catchment, *Hydrol. Earth Syst. Sci.*, 9, 139–155,  
734 <https://doi.org/10.5194/hess-9-139-2005>, 2005.

735 Salvatore, E., Bronders, J., and Batelaan, O.: Hydrological modelling of urbanized  
736 catchments: A review and future directions, *Journal of Hydrology*, 529, 62–81,  
737 <https://doi.org/10.1016/j.jhydrol.2015.06.028>, 2015.

738 Sang, L., Zhu, G., Xu, Y., Sun, Z., Zhang, Z., and Tong, H.: Effects of Agricultural  
739 Large-And Medium-Sized Reservoirs on Hydrologic Processes in the Arid  
740 Shiyang River Basin, Northwest China, *Water Resources Research*, 59,  
741 e2022WR033519, <https://doi.org/10.1029/2022WR033519>, 2023.

742 Shastri, H., Paul, S., Ghosh, S., and Karmakar, S.: Impacts of urbanization on Indian  
743 summer monsoon rainfall extremes, *J. Geophys. Res. Atmos.*, 120, 496–516,  
744 <https://doi.org/10.1002/2014JD022061>, 2015.

745 Skrzypek, G., Mydlowski, A., Dogramaci, S., Hedley, P., Gibson, J. J., and Grierson,  
746 P. F.: Estimation of evaporative loss based on the stable isotope composition of  
747 water using Hydrocalculator, *Journal of Hydrology*, 523, 781–789,  
748 <https://doi.org/10.1016/j.jhydrol.2015.02.010>, 2015.

749 Sun, G., Caldwell, P. V., and McNulty, S. G.: Modelling the potential role of forest  
750 thinning in maintaining water supplies under a changing climate across the  
751 conterminous United States: Response of Water Yield to Forest Thinning and  
752 Climate Change, *Hydrol. Process.*, 29, 5016–5030,  
753 <https://doi.org/10.1002/hyp.10469>, 2015.

754 Sun, G. and Lockaby, B. G.: Water Quantity and Quality at the Urban-Rural Interface,  
755 in: *Urban-Rural Interfaces*, edited by: Laband, D. N., Lockaby, B. G., and  
756 Zipperer, W. C., American Society of Agronomy, Soil Science Society of  
757 America, Crop Science Society of America, Inc., Madison, WI, USA, 29–48,  
758 <https://doi.org/10.2136/2012.urban-rural.c3>, 2012.

759 Sun, Z., Zhu, G., Zhang, Z., Xu, Y., Yong, L., Wan, Q., Ma, H., Sang, L., and Liu, Y.:  
760 Identifying surface water evaporation loss of inland river basin based on  
761 evaporation enrichment model, *Hydrological Processes*, 35, e14093,  
762 <https://doi.org/10.1002/hyp.14093>, 2021.

763 Talma, S, Woodborne, S. and Lorentz, S.: South African Contribution to the Rivers



764 CRP, 2012.

765 UN-Habitat: World cities report 2020: the value of sustainable urbanization,  
766 UN-Habitat, Nairobi, Kenya, 377 pp., 2020.

767 United Nations Department of Economic and Social Affairs: World Urbanization  
768 Prospects 2018: Highlights, United Nations,  
769 <https://doi.org/10.18356/6255ead2-en>, 2019.

770 Vitvar, T., Aggarwal, P. K., and Herczeg, A. L.: Global network is launched to  
771 monitor isotopes in rivers, *Eos Trans. AGU*, 88, 325–326,  
772 <https://doi.org/10.1029/2007EO330001>, 2007.

773 Vystavna, Y., Harjung, A., Monteiro, L. R., Matiatos, I., and Wassenaar, L. I.: Stable  
774 isotopes in global lakes integrate catchment and climatic controls on evaporation,  
775 *Nat Commun*, 12, 7224, <https://doi.org/10.1038/s41467-021-27569-x>, 2021.

776 Wang, B., Zhang, H., Liang, X., Li, X., and Wang, F.: Cumulative effects of cascade  
777 dams on river water cycle: Evidence from hydrogen and oxygen isotopes,  
778 *Journal of Hydrology*, 568, 604–610,  
779 <https://doi.org/10.1016/j.jhydrol.2018.11.016>, 2019.

780 Wei, W., Shi, P., Zhou, J., Feng, H., Wang, X., and Wang, X.: Environmental  
781 suitability evaluation for human settlements in an arid inland river basin: A case  
782 study of the Shiyang River Basin, *J. Geogr. Sci.*, 23, 331–343,  
783 <https://doi.org/10.1007/s11442-013-1013-y>, 2013.

784 Westra, S., Fowler, H. J., Evans, J. P., Alexander, L. V., Berg, P., Johnson, F.,  
785 Kendon, E. J., Lenderink, G., and Roberts, N. M.: Future changes to the intensity

786 and frequency of short-duration extreme rainfall, *Rev. Geophys.*, 52, 522–555,  
787 <https://doi.org/10.1002/2014RG000464>, 2014.

788 Wilson, C. and Weng, Q.: Assessing Surface Water Quality and Its Relation with  
789 Urban Land Cover Changes in the Lake Calumet Area, Greater Chicago,  
790 *Environmental Management*, 45, 1096–1111,  
791 <https://doi.org/10.1007/s00267-010-9482-6>, 2010.

792 Wing, O. E. J., Bates, P. D., Smith, A. M., Sampson, C. C., Johnson, K. A., Fargione,  
793 J., and Morefield, P.: Estimates of present and future flood risk in the  
794 conterminous United States, *Environ. Res. Lett.*, 13, 034023,  
795 <https://doi.org/10.1088/1748-9326/aaac65>, 2018.

796 Yang, L., Ni, G., Tian, F., and Niyogi, D.: Urbanization Exacerbated Rainfall Over  
797 European Suburbs Under a Warming Climate, *Geophysical Research Letters*, 48,  
798 e2021GL095987, <https://doi.org/10.1029/2021GL095987>, 2021.

799 Yang, S. L., Zhang, J., and Xu, X. J.: Influence of the Three Gorges Dam on  
800 downstream delivery of sediment and its environmental implications, Yangtze  
801 River, *Geophys. Res. Lett.*, 34, L10401, <https://doi.org/10.1029/2007GL029472>,  
802 2007.

803 Yu, D., Shi, P., Liu, Y., and Xun, B.: Detecting land use-water quality relationships  
804 from the viewpoint of ecological restoration in an urban area, *Ecological*  
805 *Engineering*, 53, 205–216, <https://doi.org/10.1016/j.ecoleng.2012.12.045>, 2013.

806 Zhang, W., Wan, Q., Zhu, G., and Xu, Y.: Distribution of soil organic carbon and  
807 carbon sequestration potential of different geomorphic units in Shiyang river

808 basin, China, *Environ Geochem Health*, 45, 4071–4086,  
809 <https://doi.org/10.1007/s10653-022-01472-w>, 2023.

810 Zhu, G., Guo, H., Qin, D., Pan, H., Zhang, Y., Jia, W., and Ma, X.: Contribution of  
811 recycled moisture to precipitation in the monsoon marginal zone: Estimate based  
812 on stable isotope data, *Journal of Hydrology*, 569, 423–435,  
813 <https://doi.org/10.1016/j.jhydrol.2018.12.014>, 2019.

814 Zhu, G., Sang, L., Zhang, Z., Sun, Z., Ma, H., Liu, Y., Zhao, K., Wang, L., and Guo,  
815 H.: Impact of landscape dams on river water cycle in urban and peri-urban areas  
816 in the Shiyang River Basin: Evidence obtained from hydrogen and oxygen  
817 isotopes, *Journal of Hydrology*, 602, 126779,  
818 <https://doi.org/10.1016/j.jhydrol.2021.126779>, 2021.